Kinetics and Thermodynamics of Mandelate Racemase Catalysis†

Martin St. Maurice and Stephen L. Bearne*

Department of Biochemistry and Molecular Biology, Dalhousie University, Halifax, Nova Scotia B3H 4H7, Canada

Received December 13, 2001; Revised Manuscript Received January 30, 2002

ABSTRACT: Mandelate racemase (EC 5.1.2.2) from *Pseudomonas putida* catalyzes the interconversion of the two enantiomers of mandelic acid with remarkable proficiency, producing a rate enhancement exceeding 15 orders of magnitude. The rates of the forward and reverse reactions catalyzed by the wild-type enzyme and by a sluggish mutant (N197A) have been studied in the absence and presence of several viscosogenic agents. A partial dependence on relative solvent viscosity was observed for values of k_{cat} and k_{cat}/K_m for the wild-type enzyme in sucrose-containing solutions. The value of k_{cat} for the sluggish mutant was unaffected by varying solvent viscosity. However, sucrose did have a slight activating effect on mutant enzyme efficiency. In the presence of the polymeric viscosogens poly(ethylene glycol) and Ficoll, no effect on k_{cat} or k_{cat}/K_m for the wild-type enzyme was observed. These results are consistent with both substrate binding and product dissociation being partially rate-determining in both directions. The viscosity variation method was used to estimate the rate constants comprising the steady-state expressions for k_{cat} and k_{cat}/K_m. The rate constant for the conversion of bound (*R*)-mandelate to bound (*S*)-mandelate (k_2) was found to be 889 ± 40 s^{-1} compared with a value of 654 ± 58 s^{-1} for k_{cat} in the same direction. From the temperature dependence of K_m (shown to equal K_S), k_2, and the rate constant for the uncatalyzed reaction [Bearne, S. L., and Wolfenden, R. (1997) *Biochemistry 36*, 1646−1656], we estimated the enthalpic and entropic changes associated with substrate binding ($\Delta H = -8.9 \pm 0.8$ kcal/mol, $T\Delta S = -4.8 \pm 0.8$ kcal/mol), the activation barrier for conversion of bound substrate to bound product ($\Delta H^{\ddagger} = +15.4 \pm 0.4$ kcal/mol, $T\Delta S^{\ddagger} = +2.0 \pm 0.1$ kcal/mol), and transition state stabilization ($\Delta H_{tx} = -22.9 \pm 0.8$ kcal/mol, $T\Delta S_{tx} = +1.8 \pm 0.8$ kcal/mol) during mandelate racemase-catalyzed racemization of (*R*)-mandelate at 25 °C. Although the high proficiency of mandelate racemase is achieved principally by enthalpic reduction, there is also a favorable and significant entropic contribution.

Mandelate racemase (EC 5.1.2.2) from *Pseudomonas putida* catalyzes the Mg^{2+}-dependent 1,1-proton transfer that interconverts the enantiomers of mandelic acid (*1*−*3*). Catalysis proceeds via a two-base mechanism, with His 297 and Lys 166 abstracting the α-proton from (*R*)-mandelate and (*S*)-mandelate, respectively (*4*−*6*). In addition, site-directed mutagenesis experiments have revealed that Glu 317 acts as a general acid catalyst (*7*) and Asn 197 interacts with the α-hydroxy group of mandelate to facilitate stabilization of the transition state (*8*). Mandelate racemase has been studied as a paradigm for enzymes that catalyze rapid hydrogen−carbon bond cleavage of carbon acids with relatively high pK_a values (*9*−*12*). Like all enzymes, mandelate racemase provides rate enhancements by stabilizing the transition state of a reaction relative to the ground state. Indeed, mandelate racemase is extremely proficient at discriminating between the substrate in the ground state and the altered substrate in the transition state, binding the latter with an apparent association constant equal to 5×10^{18} M^{-1} and reducing the activation barrier for the reaction by 26 kcal/mol (*13*).

The proficiency of an enzyme is a measure of transition state stabilization and is defined as the reciprocal of the virtual dissociation constant of the enzyme−substrate complex in the transition state (K_{tx}) as defined by eq 1 (*14*). The enthalpic and entropic contributions to the free energy of transition state stabilization can be determined from the temperature effects on enzyme proficiency. Such studies have been conducted with only a limited number of enzymes including fumarase, ribonuclease A, and carbonic anhydrase (*15*) and most thoroughly for cytidine deaminase (*16*). For these enzymes, transition state stabilization is largely enthalpy-based (*17*). Our interest in developing a detailed understanding of how enzymes achieve catalysis has led us to investigate the enthalpic and entropic contributions to mandelate racemase proficiency.

$$K_{tx} = k_{non}/(k_{cat}/K_S) \quad (1)$$

To obtain a meaningful value of K_{tx}, either the dissociation constant for the enzyme−substrate complex in the ground state (K_S) must be determined or the Michaelis constant (K_m) must be shown to approximate K_S. In addition, k_{cat} must describe the chemical step for which the rate constant of the corresponding nonenzymatic reaction (k_{non}) has been determined. However, this is often not the case when substrate binding or product release is partially rate-determining (*18*, *19*) or when the enzyme-catalyzed and nonenzymatic reac-

† This work was supported by the Natural Sciences and Engineering Research Council of Canada (NSERC). M.St.M. is the recipient of an NSERC postgraduate scholarship.

* To whom correspondence should be addressed: phone, (902) 494-1974; fax, (902) 494-1355; e-mail, sbearne@is.dal.ca.

10.1021/bi016044h CCC: $22.00
Published on Web 03/03/2002

tions do not proceed via the same mechanism. These caveats have been discussed in detail elsewhere (*18*, *19*).

For mandelate racemase, the substrate kinetic deuterium isotope effect (k_{cat}^{H}/k_{cat}^{D}) for proton abstraction from (*R*)-mandelate is ~3.2 (*7*, *20*), and the solvent deuterium isotope effect on k_{cat} is ~2.3 (*7*). These observations led Gerlt and co-workers (*7*) to suggest that both proton abstraction from the substrate and proton delivery to form the product are each partially rate-determining and that substrate association and product dissociation are faster than the proton transfer reactions. The possibility remains, however, that diffusive processes such as substrate association or product dissociation are also partially rate-determining. Indeed, partial diffusion control has been observed for several enzymes including β-glucosidase (*21*), alkaline phosphatase (*22*), 1-aminocyclopropane-1-carboxylate synthase (*23*), ribonuclease T_1 (*24*), subtilisin BPN′ (*25*), and chorismate mutase (*26*) for which the values of k_{cat}/K_m are on the order of 10^5-10^6 (cf. k_{cat}/K_m for mandelate racemase $\approx 10^6$ M^{-1} s^{-1}), well below the theoretical limit of 10^8-10^{10} M^{-1} s^{-1} for a diffusion-limited enzyme-catalyzed reaction (*27*).

In the present work, we show that mandelate racemase displays a partial viscosity dependence indicating that the chemical step is not completely rate-determining. Using kinetic measurements obtained at various solvent viscosities, we determined the values of the rate constants that comprise k_{cat} and k_{cat}/K_m in both reaction directions. In addition, we used the alternative substrate, (*S*)-*p*-nitromandelate, in combination with (*R*,*S*)-mandelate to demonstrate that $K_m \approx K_S$ for both (*R*)- and (*S*)-mandelate. This information, combined with measurements of the temperature dependence of both the catalytic efficiency of the enzyme-catalyzed chemical step and the rate constant for the corresponding nonenzymatic reaction, permitted us to determine the temperature dependence of K_{tx}. Herein, we report the enthalpy and entropy changes associated with substrate binding, the activation barrier for conversion of bound substrate to bound product, and transition state stabilization during mandelate racemase-catalyzed racemization of (*R*)-mandelate. Although the high proficiency of mandelate racemase is achieved principally by enthalpic reduction, there is also a favorable and significant entropic contribution.

MATERIALS AND METHODS

Acetonitrile (HPLC grade) and poly(ethylene glycol) (PEG,[1] M_r 6000−7500) were purchased from Fisher Scientific (Nepean, Ontario, Canada). Sucrose and glycerol were purchased from BDH, Inc. (Toronto, Ontario, Canada). Racemic, (*R*)-, and (*S*)-mandelic acid, 4-nitrobenzaldehyde, (*R*)-(+)-α-methylbenzylamine, D-(+)-trehalose, Ficoll 400, and all other reagents were purchased from Sigma-Aldrich (Oakville, Ontario, Canada). Recombinant mandelate racemase from *P. putida* was overexpressed in and purified from *Escherichia coli* strain BL21(DE3) cells transformed with a pET15b plasmid (Novagen, Madison, WI) containing the mandelate racemase gene. This construct encodes the mandelate racemase gene product with an N-terminal hexahistidine tag (MGSSHHHHHHSSGLVPRGSHM$_1$ ... mandelate racemase). The enzyme was overexpressed and purified using metal ion affinity chromatography as described previously (*8*). [The presence of the histidine tag does not influence the values of k_{cat} and K_m for the recombinant enzyme (*28*).] The N197A mutant of mandelate racemase was also overexpressed and purified as described previously (*8*). Circular dichroism (CD) assays were conducted using a JASCO J-810 spectropolarimeter. The CD spectrum (200−260 nm) of mandelate racemase obtained in the presence of sucrose (35%) was corrected by subtracting the CD spectrum arising solely from the sucrose (35%).

Resolution of (S)-p-Nitromandelate. (*R*,*S*)-*p*-Nitromandelic acid was prepared by reacting *p*-nitrobenzaldehyde with trimethylsilyl cyanide in the presence of a catalytic amount of zinc iodide as described by Westkaemper and Hanzlik (*29*). (*S*)-*p*-Nitromandelate was resolved in a series of small batch preparations (*30*). In each batch, (*R*)-(+)-α-methylbenzylamine (0.30 g, 2.5 mmol) was added to a boiling solution of (*R*,*S*)-*p*-nitromandelic acid (0.5 g, 2.5 mmol) in ethanol (10 mL). The solution was allowed to cool to room temperature, and crystallization occurred within 4 h. The α-methylbenzylammonium salt was collected using suction filtration and washed three times with cold ethanol (10 mL). This salt (0.5 g) was recrystallized three times from hot ethanol (10 mL). Recrystallization solutions were stored at 4 °C, and if no crystals formed within 24 h, acetone (2−3 drops) was added to promote crystallization. The isolated salt was then dissolved in water and converted to its sodium salt by passage through a column containing AG 50W-X8 (Na^+ form). The column was eluted with water, and fractions containing *p*-nitromandelate were pooled and lyophilized. These small batch recrystallizations were performed repeatedly, starting with a total of 8 g of (*R*,*S*)-*p*-nitromandelate and giving a final yield of 0.36 g of sodium (*S*)-*p*-nitromandelate (8%). The resolution was monitored using HPLC on a Chirex D-penicillamine column (150 × 4.6 mm; Phenomenex, Torrance, CA). (*R*)- and (*S*)-*p*-nitromandelate were eluted under isocratic conditions using 15% acetonitrile in aqueous $CuSO_4$ (2 mM) at a flow rate of 1.0 mL/min over a period of 250 min. The solvent was degassed prior to use. A Waters 510 pump and 486 controller were used for solvent delivery. Injections were made using a Rheodyne 7725i sample injector fitted with a 50 μL injection loop. The eluted enantiomers of *p*-nitromandelate were detected by monitoring the absorbance at 254 nm using a Waters 486 tuneable absorbance detector. Peak areas were determined by integration of the resulting chromatograms using PeakSimple software from Mandel Scientific (Guelph, Ontario, Canada). (*S*)-(+)- and (*R*)-(−)-*p*-nitromandelate eluted with retention times of approximately 190 and 230 min, respectively. The absolute stereochemistry was assigned using the optical rotations reported by Westkaemper and Hanzlik (*29*). The relative peak areas indicated that the final product from the resolution was 98% (*S*)-*p*-nitromandelate (i.e., 99% ee).

Viscosity Effects. Both monomeric viscosogens (sucrose, trehalose, and glycerol) and polymeric viscosogens (PEG and Ficoll 400) were used in the present study. Stock solutions of these viscosogenic reagents were prepared at twice the desired final concentration, diluted 1:1 with HEPES buffer (0.2 M, pH 7.5) containing $MgCl_2$ (6.6 mM), and passed through a sintered glass filter to remove any suspended material. The kinematic viscosities were subsequently mea-

[1] Abbreviations: BSA, bovine serum albumin; CD, circular dichroism; HEPES, 4-(2-hydroxyethyl)piperazine-1-ethanesulfonic acid; PEG, poly(ethylene glycol).

sured in triplicate using a Cannon-Fenske viscometer at 25 °C and using HEPES buffer (0.1 M, pH 7.5) containing $MgCl_2$ (3.3 mM) as the reference. Solution densities were determined gravimetrically at 25 °C, and the relative solvent viscosities ($\eta_{rel} = \eta/\eta^0$, where the superscript refers to the reaction in HEPES buffer in the absence of added viscosogen) of the viscosogen-containing buffer solutions were calculated from the product of these densities (ρ) and the measured kinematic viscosities (η/ρ). Relative viscosities were approximately 1.32, 1.88, 2.48, 3.06, and 3.42 for 10%, 20%, 27.5%, 32.5%, and 35% (w/v) sucrose solutions, respectively; $\eta_{rel} = 1.73$, 2.10, 2.73, and 3.43 for 20%, 25%, 30%, and 35% (w/v) trehalose solutions, respectively; $\eta_{rel} = 1.44$, 1.69, 2.09, 2.73, 3.20, and 4.01 for 10%, 15%, 20%, 25%, 27.5%, and 30% (w/v) glycerol solutions, respectively; $\eta_{rel} = 1.22$, 1.89, 2.81, and 4.03 for 1.5%, 3%, 6%, and 8% (w/v) Ficoll 400 solutions, respectively; $\eta_{rel} = 1.61$, 2.50, 5.37, and 8.49 for 2.5%, 5%, 6%, and 7.5% (w/v) PEG solutions, respectively.

Kinetic measurements were conducted using the CD assay at 262 nm described by Sharp et al. (*31*). Reaction mixtures were prepared in rectangular quartz cuvettes with a 1 cm light path. Typically, 950 μL of (*R*)- or (*S*)-mandelate (0.5−20.0 mM) in HEPES buffer (0.2 M, pH 7.5) containing $MgCl_2$ (6.6 mM) was mixed with 950 μL of the viscosogen-containing stock solution (prepared at twice the desired final concentration). The reaction was initiated by addition of 100 μL of either wild-type mandelate racemase (5 μg/mL) or the N197A mutant (468 μg/mL) in HEPES buffer (0.1 M, pH 7.5) containing $MgCl_2$ (3.3 mM) and bovine serum albumin (BSA, 0.1%). All kinetic experiments were conducted in the plateau region of the pH−k_{cat} (*6*) and pH−K_m (*8*) profiles for the enzyme-catalyzed racemization reaction and well above the pK_a value of 3.41 for mandelic acid (*32*). Hence, the effects of both the viscosogenic cosolutes and changes in temperature (vide infra) on the pH profiles of the enzyme-catalyzed reaction are expected to be negligible.

Temperature Effects. For each reaction conducted at a given temperature, a stock solution of (*R*)-mandelate (20 mM) was prepared in HEPES buffer (0.2 M, pH 7.5) containing $MgCl_2$ (6.6 mM). The pH of both the buffer and the (*R*)-mandelate stock solution was adjusted at each assay temperature to 7.5 relative to thermostated standards. The relative viscosities for the sucrose solutions at 10, 15, 20, 25, 30, 35, 40, and 45 °C were calculated from the product of the kinematic viscosities measured at each of these temperatures and the densities of the sucrose solutions at each temperature [calculated using the equation reported by Bubnik et al. (*33*)]. Mandelate racemase activity was assayed at each of these temperatures using the CD assay. The molar ellipticity for (*R*)-mandelate did not change over this temperature range. All assays were conducted in rectangular quartz cuvettes with a 1.0 cm light path. Additional stock solutions of (*R*)-mandelate (0.5−20 mM) were prepared by dilution of the stock 20 mM solution with HEPES buffer (0.2 M, pH 7.5) containing $MgCl_2$ (6.6 mM). Substrate solutions (1.900 mL) were prepared by mixing 950 μL of the stock (*R*)-mandelate solutions with 950 μL of the desired sucrose-containing stock solution to yield (*R*)-mandelate assay concentrations ranging between 0.25 and 10.0 mM in HEPES buffer (0.1 M, pH 7.5) containing $MgCl_2$ (3.3 mM). Each substrate solution was incubated for 5 min in a water bath at the desired temperature prior to initiation of the reaction by addition of mandelate racemase (100 μL, 1.0−12.0 μg/mL) in HEPES buffer (0.1 M, pH 7.5) containing $MgCl_2$ (3.3 mM) and BSA (0.1%). The progress of the reaction was monitored by following the change in ellipticity at 262 nm. The reaction was maintained at the desired temperature using a thermostated rectangular cell holder with a remote temperature probe connected to a Neslab RTE-111 water bath.

Determination of K_S. The value of K_S for (*R*)- and (*S*)-mandelate was determined by assaying the activity of mandelate racemase with the alternative substrate (*S*)-*p*-nitromandelate in the presence of the "competitive inhibitor", (*R*,*S*)-mandelate (see Results). Mandelate racemase activity was assayed using a CD assay similar to that described by Sharp et al. (*31*); however, the CD signal was monitored at 232 nm over 5 min. Final concentrations of (*S*)-*p*-nitromandelate were 1.0, 1.5, 2.0, 2.5, 3.0, and 3.5 mM. Final concentrations of (*R*,*S*)-mandelate were 0.0, 0.5, 1.0, and 2.0 mM. Assays were conducted at 25 °C in HEPES buffer (0.1 M, pH 7.5) containing $MgCl_2$ (3.3 mM) using a rectangular quartz cuvette with a 0.1 cm light path. Reactions were initiated by addition of mandelate racemase (50 μL, 2.0 μg/mL, 0.1% BSA) to a solution (200 μL) containing both (*S*)-*p*-nitromandelate (substrate) and (*R*,*S*)-mandelate (inhibitor) that had been preincubated at 25 °C for 5 min. [Initiation of the reaction with (*S*)-*p*-nitromandelate following a 5 min preincubation of 2 μg/mL mandelate racemase with (*R*,*S*)-mandelate did not change the observed initial velocity.] Apparent V_{max}/K_m values were determined in triplicate at each concentration of (*R*,*S*)-mandelate.

Data Analysis. The values of V_{max} and K_m were determined from plots of the initial velocity (v_i) versus substrate concentration ([S]) by fitting the data to eq 2 using nonlinear regression analysis and the program EnzymeKinetics v1.5b5 (Trinity Software, Plymouth, NH). Kinetic constants were determined in duplicate for the temperature dependence experiments and in triplicate for all other experiments. The reported errors are the standard deviations. Protein concentrations were determined using the Bio-Rad protein assay (Bio-Rad Laboratories, Mississauga, Ontario, Canada) with BSA standards, and k_{cat} values were obtained by dividing V_{max} values by the total enzyme concentration using M_r 40728.

$$v_i = \frac{V_{max}[S]}{K_m + [S]} \quad (2)$$

RESULTS

Viscosity Effects. The rates of external steps such as those occurring during enzyme−substrate association and enzyme−product dissociation are expected to be inversely proportional to the solvent microviscosity while the rates of internal processes (i.e., those occurring within enzyme−substrate complexes) are expected to be independent of solvent microviscosity (*22*−*26*, *34*−*45*). To determine whether substrate binding or product release is rate-determining for the reaction catalyzed by mandelate racemase, we employed the viscosity variation method (*36*) to investigate the dependence of k_{cat} and k_{cat}/K_m on viscosity in both the $R \rightarrow S$ (Table 1) and $S \rightarrow R$ (Table 2) reaction directions. A partial

Table 1: Dependence of $k_{cat}^{R\rightarrow S}$ and $(k_{cat}/K_m)^{R\rightarrow S}$ on Viscosity for Wild-Type and N197A Mandelate Racemases

viscosogen [% (w/v)]	η/η^0	$k_{cat}^{R\rightarrow S}$ (s^{-1})	$(k_{cat}/K_m)^{R\rightarrow S}$ ($\times 10^5$ M^{-1} s^{-1}) observed	corrected[a]
Sucrose (wild type)				
0.0	1.00	654 ± 58	6.41 ± 0.57	6.41 ± 0.57
10.0	1.32	556 ± 32	5.90 ± 1.20	5.63 ± 1.14
20.0	1.88	506 ± 43	5.69 ± 0.60	5.05 ± 0.53
27.5	2.48	446 ± 25	6.21 ± 0.56	5.03 ± 0.45
32.5	3.06	399 ± 26	5.76 ± 0.62	4.42 ± 0.48
35.0	3.42	370 ± 35	6.21 ± 1.91	4.49 ± 1.38
Sucrose (N197A)				
0.0	1.00	17.9 ± 1.2	0.027 ± 0.005	0.027 ± 0.005
10.0	1.34	18.3 ± 3.1	0.029 ± 0.006	0.028 ± 0.006
20.0	1.88	19.7 ± 3.7	0.031 ± 0.009	0.027 ± 0.008
27.5	2.56	18.2 ± 2.0	0.039 ± 0.008	0.029 ± 0.006
32.5	3.18	20.2 ± 4.4	0.043 ± 0.013	0.028 ± 0.008
35.0	3.69	21.2 ± 5.3	0.043 ± 0.014	0.025 ± 0.008
Trehalose (wild type)				
0.0	1.00	779 ± 45	8.38 ± 1.78	
20.0	1.73	663 ± 22	7.45 ± 1.49	
25.0	2.10	614 ± 8	8.94 ± 0.60	
30.0	2.73	506 ± 27	9.85 ± 1.81	
35.0	3.43	435 ± 16	7.72 ± 2.02	

[a] The slope of relative $(k_{cat}/K_m)^{R\rightarrow S}$ vs η/η^0 for the N197A enzyme (slope = -0.163 ± 0.002) in the presence of sucrose was used to correct the observed relative $(k_{cat}/K_m)^{R\rightarrow S}$ values for the wild-type enzyme using the equation $[(k_{cat}/K_m)^0/(k_{cat}/K_m)^\eta]_{corr} = [(k_{cat}/K_m)^0/(k_{cat}/K_m)^\eta]_{obs} + 0.16(\eta/\eta^0 - 1)$, based on refs *35* and *46*.

Table 2: Dependence of $k_{cat}^{R\rightarrow S}$ and $(k_{cat}/K_m)^{S\rightarrow R}$ on Viscosity for Wild-Type and N197A Mandelate Racemases

viscosogen [% (w/v)]	η/η^0	$k_{cat}^{R\rightarrow S}$ (s^{-1})	$(k_{cat}/K_m)^{S\rightarrow R}$ ($\times 10^5$ M^{-1} s^{-1}) observed	corrected[a]
Sucrose (wild type)				
0.0	1.00	491 ± 14	6.11 ± 0.64	6.11 ± 0.64
10.0	1.32	464 ± 39	6.10 ± 1.20	5.79 ± 1.14
20.0	1.88	389 ± 35	6.63 ± 1.05	5.71 ± 0.90
27.5	2.48	349 ± 42	6.04 ± 1.52	4.85 ± 1.22
32.5	3.06	314 ± 42	5.79 ± 2.15	4.36 ± 1.62
35.0	3.42	291 ± 13	5.74 ± 0.67	4.15 ± 0.48
Sucrose (N197A)				
0.0	1.00	4.4 ± 0.3	0.025 ± 0.009	0.025 ± 0.009
10.0	1.34	4.5 ± 0.2	0.031 ± 0.013	0.029 ± 0.012
20.0	1.88	4.3 ± 0.2	0.029 ± 0.009	0.025 ± 0.008
27.5	2.56	4.2 ± 0.3	0.039 ± 0.009	0.028 ± 0.006
32.5	3.18	4.1 ± 0.7	0.034 ± 0.026	0.023 ± 0.017
35.0	3.69	4.0 ± 0.4	0.048 ± 0.008	0.026 ± 0.004

[a] The slope of relative $(k_{cat}/K_m)^{S\rightarrow R}$ vs η/η^0 for the N197A enzyme (slope = -0.174 ± 0.003) in the presence of sucrose was used to correct the observed relative $(k_{cat}/K_m)^{S\rightarrow R}$ values for the wild-type enzyme using the equation $[(k_{cat}/K_m)^0/(k_{cat}/K_m)^\eta]_{corr} = [(k_{cat}/K_m)^0/(k_{cat}/K_m)^\eta]_{obs} + 0.17(\eta/\eta^0 - 1)$, based on refs *35* and *46*.

viscosity dependence was observed for relative values of k_{cat} (i.e., k_{cat}^0/k_{cat}^η) in the presence of both sucrose (Figures 1A and 2A) and trehalose (Figure 3A), suggesting that product release is partially rate-determining for mandelate racemase catalysis in both reaction directions.

Studies using the viscosity variation method are subject to a variety of potential complications which must be considered before the results can be interpreted in terms of diffusion-controlled processes. The high concentrations of polyhydroxylated compounds employed as viscosogenic cosolutes can have a variety of diffusion-unrelated effects including alteration of the free energy of both unbound and bound species, alteration of the pH profile for the kinetic

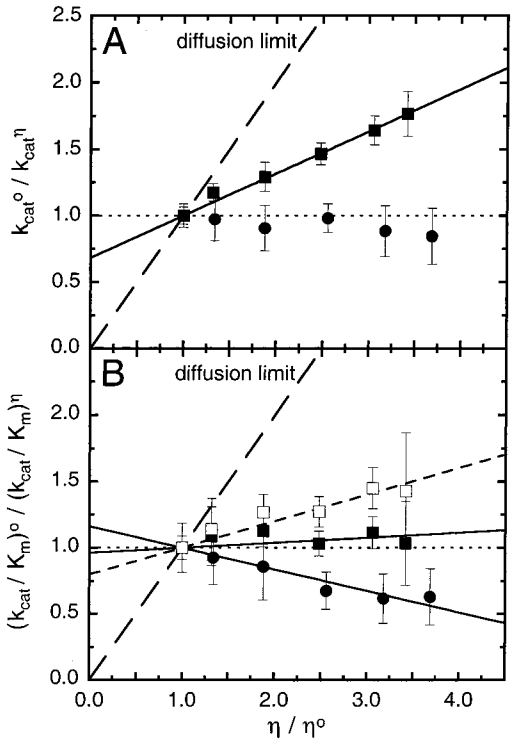

FIGURE 1: Dependence of relative kinetic parameters for the racemization of (*R*)-mandelate on relative solvent viscosity. The values of relative k_{cat} (A) and relative k_{cat}/K_m (B) for both wild-type mandelate racemase (■) and N197A (●) were determined at 25 °C at varying values of η_{rel} using sucrose as the viscosogen. The relative k_{cat} values for wild-type mandelate racemase were proportional to η_{rel} (slope = 0.288 ± 0.005), while the relative k_{cat} values for the N197A mutant showed no viscosity dependence in the presence of sucrose. The relative k_{cat}/K_m values for the N197A mutant varied inversely with η_{rel} (slope = -0.163 ± 0.002). Relative k_{cat}/K_m values for the wild-type enzyme that have been corrected for diffusion-unrelated effects (see Table 1) are also shown (□). The slope of the corrected line (short dashes) is 0.186 ± 0.004.

parameters (see Materials and Methods), perturbations in solvent structure, alteration of substrate and enzyme conformations, and inhibition or activation of the enzymatic reaction. Assurances against the occurrence of effects that do not involve diffusive processes can be obtained by (a) demonstrating that similar kinetic behavior is observed when different monomeric viscosogens (which affect both solvent microviscosity and macroviscosity) are used, (b) demonstrating that polymeric viscosogens (which affect only the solvent macroviscosity) do not alter the kinetic parameters, and (c) characterizing the effect of viscosogens on the activity of a "sluggish" mutant (*35*). In the present work, the viscosity dependence observed for the relative k_{cat} values was similar in the presence of both sucrose and trehalose (Figures 1−3). The relative k_{cat} value also exhibited a viscosity dependence in the presence of glycerol. However, this dependence was curvilinear, especially at relative viscosities greater than 2.5 (Figure 3A). Glycerol, a relatively small molecule, may be acting as an inhibitor of the enzyme in addition to mediating solvent viscosity effects and, therefore, was not considered to be suitable as a viscosogen in the present study. Such aberrant behavior of glycerol in solvent viscosity studies has been reported for several enzymes, including carbonic anhydrase (*41*), alkaline phosphatase (*22*), and acetylcholinesterase (*34*). In the presence of the polymeric viscosogens Ficoll and PEG, no viscosity dependence was observed for

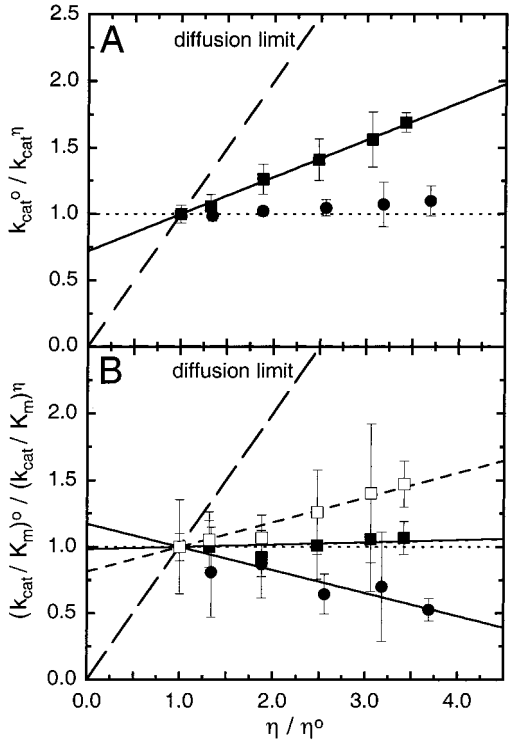

FIGURE 2: Dependence of relative kinetic parameters for the racemization of (*S*)-mandelate on relative solvent viscosity. The values of relative k_{cat} (A) and relative k_{cat}/K_m (B) for both wild-type mandelate racemase (■) and N197A (●) were determined at 25 °C at varying values of η_{rel} using sucrose as the viscosogen. The relative k_{cat} values for wild-type mandelate racemase were proportional to η_{rel} (slope = 0.259 ± 0.002), while the relative k_{cat} values for the N197A mutant showed no viscosity dependence in the presence of sucrose. The relative k_{cat}/K_m values for the N197A mutant varied inversely with relative viscosity (slope = −0.174 ± 0.003). Relative k_{cat}/K_m values for the wild-type enzyme that have been corrected for diffusion-unrelated effects (see Table 1) are also shown (□). The slope of the corrected line (short dashes) is 0.172 ± 0.002.

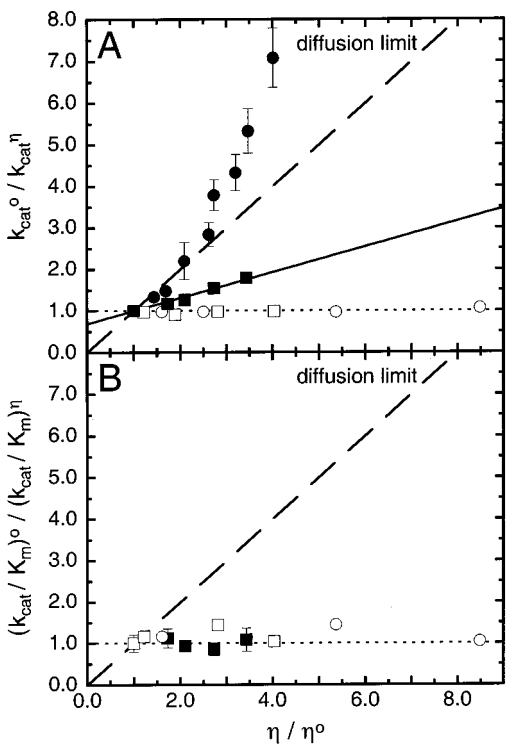

FIGURE 3: Dependence of relative kinetic parameters for mandelate racemase-catalyzed racemization of (*R*)-mandelate on relative solvent viscosity in the presence of various viscosogens. The values of relative k_{cat} (A) and relative k_{cat}/K_m (B) for wild-type mandelate racemase are shown in the presence of the monomeric viscosogens glycerol (●) and trehalose (■) and the polymeric viscosogens Ficoll 400 (□) and PEG (○). The slope of the solid line in (A) is 0.309 ± 0.007.

Scheme 1

$$\text{E + (}R\text{)-man} \underset{k_{-1}}{\overset{k_1}{\rightleftharpoons}} \text{E•(}R\text{)-man} \underset{k_{-2}}{\overset{k_2}{\rightleftharpoons}} \text{E•(}S\text{)-man} \underset{k_{-3}}{\overset{k_3}{\rightleftharpoons}} \text{E + (}S\text{)-man}$$

relative values of k_{cat} and k_{cat}/K_m up to a relative viscosity of 8.4 (Figure 3). In addition, the relative k_{cat} value for the sluggish mutant, N197A ($k_{cat}/K_m = 3.1 \times 10^3$ M^{-1} s^{-1}), for which the proton abstraction step is expected to be solely rate-determining (*8*), displays no viscosity dependence (Figures 1A and 2A). Finally, the CD spectra of wild-type mandelate racemase in the absence and presence of 35% sucrose ($\eta_{rel} = 3.42$) are indistinguishable (data not shown). This suggests that sucrose does not significantly alter the secondary structure of the enzyme, although slight changes in enzyme conformation in the presence of the viscosogen cannot be ruled out. These observations are all consistent with the observed viscosity dependence of k_{cat} being a diffusion-related process.

A slight dependence of the relative catalytic efficiency ($(k_{cat}/K_m)^0/(k_{cat}/K_m)^\eta$) on viscosity was observed for wild-type mandelate racemase in the presence of sucrose (Figures 1B and 2B) and trehalose (Figure 3B). The larger errors associated with the k_{cat}/K_m data, relative to the k_{cat} data, were the result of difficulty in accurately measuring reaction velocities at low substrate concentrations in the presence of viscosogens. For the N197A enzyme, a slight activating effect was observed in the presence of sucrose (increased k_{cat}/K_m values in Tables 1 and 2). Such activation is not unprecedented (*34*, *42*, *43*), and the observed k_{cat}/K_m values for the wild-type enzyme must be corrected for this minor diffusion-unrelated effect as described in Tables 1 and 2 (*35*, *46*). The partial viscosity dependence of the corrected relative k_{cat}/K_m values in the $R \rightarrow S$ and $S \rightarrow R$ directions (Figures 1B and 2B) suggests that substrate binding is also partially rate-determining for mandelate racemase catalysis in both reaction directions.

The viscosity dependence of an enzyme-catalyzed reaction may be used to estimate the rate constants for various steps along the reaction pathway (*24*−*26*, *34*, *36*, *37*, *39*, *40*, *42*, *44*, *45*). Scheme 1 shows a kinetic mechanism that describes the reaction catalyzed by mandelate racemase. Utilizing sucrose as the viscosogen, we have used the viscosity dependence of mandelate racemase-catalyzed racemization in both the $R \rightarrow S$ and $S \rightarrow R$ directions to estimate each of the rate constants defined in Scheme 1. The viscosity dependence for $1/k_{cat}$ (Figure 4A) and K_m/k_{cat} (Figure 4B) were determined in both reaction directions at 25 °C. Following a method similar to that described previously (*26*, *36*), we have used the steady-state initial velocity expressions for reactions in the $R \rightarrow S$ [i.e., k_{-3}[(*S*)-man] ≈ 0] and $S \rightarrow R$ [i.e., k_1[(*R*)-man] ≈ 0] directions to derive expressions for k_{cat} and k_{cat}/K_m (eqs 3−6). The rate constants k_1, k_{-1}, k_3, and k_{-3} are inversely proportional to the solvent microviscosity (i.e., $k_i = k_i^0/\eta_{rel}$, where $i = 1$, −1, 3, or −3, and η_{rel}

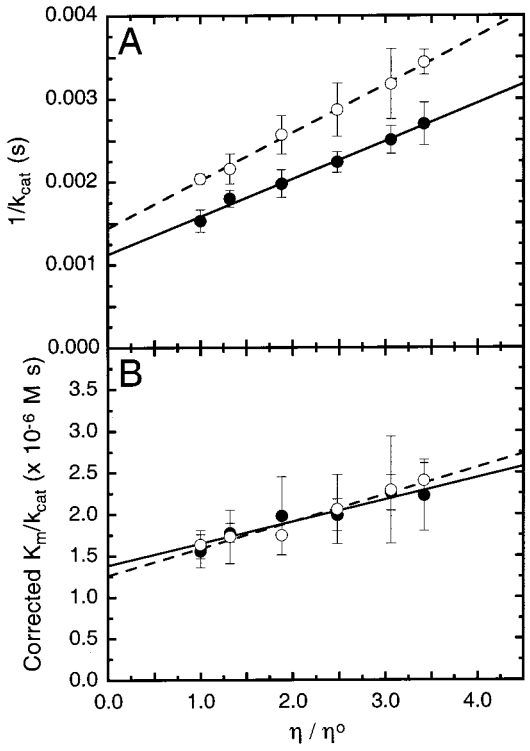

FIGURE 4: Dependence of $1/k_{cat}$ (A) and corrected K_m/k_{cat} (B) on relative solvent viscosity for the racemization of (*R*)-mandelate (●) and (*S*)-mandelate (○) by mandelate racemase in sucrose-containing buffers at 25 °C. The corrected values of K_m/k_{cat} were obtained as described in Table 1.

$= \eta/\eta^0$). Therefore, eqs 3−6 may be expressed in terms of η/η^0 as shown in eqs 7−10. The plot of $1/k_{cat}$ versus η/η^0

$$k_{cat}^{R\rightarrow S} = \frac{k_2k_3}{k_{-2} + k_2 + k_3} \quad (3)$$

$$k_{cat}^{S\rightarrow R} = \frac{k_{-1}k_{-2}}{k_{-1} + k_{-2} + k_2} \quad (4)$$

$$\frac{k_{cat}^{R\rightarrow S}}{K_m^{(R)-man}} = \frac{k_1k_2k_3}{k_{-1}k_{-2} + k_{-1}k_3 + k_2k_3} \quad (5)$$

$$\frac{k_{cat}^{S\rightarrow R}}{K_m^{(S)-man}} = \frac{k_{-1}k_{-2}k_{-3}}{k_{-1}k_{-2} + k_{-1}k_3 + k_2k_3} \quad (6)$$

$$\frac{1}{k_{cat}^{R\rightarrow S}} = \left(\frac{k_{-2} + k_2}{k_2k_3^0}\right)\frac{\eta}{\eta^0} + \frac{1}{k_2} \quad (7)$$

$$\frac{K_m^{(R)-man}}{k_{cat}^{R\rightarrow S}} = \frac{1}{k_1^0}\left(\frac{k_{-1}^0k_{-2}}{k_2k_3^0} + 1\right)\frac{\eta}{\eta^0} + \frac{k_{-1}^0}{k_1^0k_2} \quad (8)$$

$$\frac{1}{k_{cat}^{S\rightarrow R}} = \left(\frac{k_{-2} + k_2}{k_{-1}^0k_{-2}}\right)\frac{\eta}{\eta^0} + \frac{1}{k_{-2}} \quad (9)$$

$$\frac{K_m^{(S)-man}}{k_{cat}^{S\rightarrow R}} = \frac{1}{k_{-3}^0}\left(\frac{k_2k_3^0}{k_{-1}^0k_{-2}} + 1\right)\frac{\eta}{\eta^0} + \frac{k_3^0}{k_{-2}k_{-3}^0} \quad (10)$$

(Figure 4A) has an intercept equal to $1/k_2$ in the $R \rightarrow S$ direction and $1/k_{-2}$ in the $S \rightarrow R$ direction. The values for k_2 and k_{-2} can be used to calculate k_3^0 and k_{-1}^0 from the slopes of these plots. Both the intercepts and slopes from plots of K_m/k_{cat} versus η/η^0 in the $R \rightarrow S$ and $S \rightarrow R$ directions (Figure 4B), combined with the values of the rate constants determined from the $1/k_{cat}$ versus η/η^0 plots, can be used to estimate k_1^0 and k_{-3}^0, respectively. The values for all of the rate constants defined in Scheme 1 are given in Table 3.

Table 3: Rate Constants for the Reaction Catalyzed by Mandelate Racemase

	rate constant	app $\Delta G^{\ddagger}$ (kcal mol^{-1}) at 25 °C
k_1	$(3.21 \pm 0.31) \times 10^6$ M^{-1} s^{-1} [a]	8.6 ± 0.8[c]
	$(6.73 \pm 0.80) \times 10^6$ M^{-1} s^{-1} [b]	8.2 ± 1.0[c]
k_{-1}	3948 ± 199 s^{-1}	12.5 ± 0.6
k_2	889 ± 40 s^{-1}	13.4 ± 0.6
k_{-2}	693 ± 20 s^{-1}	13.6 ± 0.4
k_3	3896 ± 276 s^{-1}	12.6 ± 0.9
k_{-3}	$(4.46 \pm 0.45) \times 10^6$ M^{-1} s^{-1} [a]	8.4 ± 0.8[c]
	$(6.87 \pm 0.64) \times 10^6$ M^{-1} s^{-1} [b]	8.1 ± 0.8[c]

[a] Values calculated from the *y*-intercepts of $(K_m/k_{cat})_{corr}$ vs η_{rel} (Figure 4B). [b] Values calculated from the slopes of $(K_m/k_{cat})_{corr}$ vs η_{rel} (Figure 4B). [c] Values calculated for a standard state of 1 M.

Scheme 2

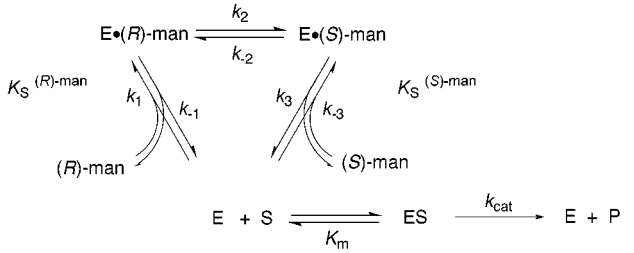

Determination of K_S Using an Alternative Substrate. All kinetic assays with (*S*)-*p*-nitromandelate were conducted at 232 nm where (*S*)-*p*-nitromandelate gave a strong CD signal ($[\theta]_{232} = 8910$ deg cm^2 dmol^{-1}) with a relatively low absorbance. Nevertheless, the absorbance of (*S*)-*p*-nitromandelate at 232 nm did restrict assays to substrate concentrations less than 15 mM. Mandelate racemase appears to have a very low affinity for (*S*)-*p*-nitromandelate since saturation kinetics were not observed at substrate concentrations up to 15 mM. Although this precluded measurements of individual K_m and V_{max} values, V_{max}/K_m values for (*S*)-*p*-nitromandelate were obtained from the initial rates observed at substrate concentrations less than 3 mM (i.e., where $[S] \ll K_m$ and $v_i = V_{max}[S]/K_m$). Mandelate racemase catalyzes the racemization of (*S*)-*p*-nitromandelate less efficiently [$k_{cat}/K_m = (4.08 \pm 0.05) \times 10^4$ M^{-1} s^{-1}] than it catalyzes the racemization of (*S*)-mandelate [$k_{cat}/K_m = (7.2 \pm 0.5) \times 10^5$ M^{-1} s^{-1} (*8*)].

The substrate dissociation constants for (*R*)-mandelate ($K_S^{(R)-man}$) and (*S*)-mandelate ($K_S^{(S)-man}$) were determined kinetically by conducting assays with (*S*)-*p*-nitromandelate as the substrate and using (*R*,*S*)-mandelate as a competitive inhibitor of the reaction. Equation 11 gives the velocity expression describing classical competitive inhibition where [S] is the concentration of (*S*)-*p*-nitromandelate. The apparent inhibition constant for (*R*,*S*)-mandelate (K_i^{app}) was calculated from plots of the observed K_m/V_{max} values against the concentration of (*R*,*S*)-mandelate as shown in Figure 5. The kinetic mechanism describing such inhibition is shown in Scheme 2, and the corresponding steady-state initial velocity expression [where d[(*R*)-man]/dt = d[(*S*)-man]/dt = 0] for

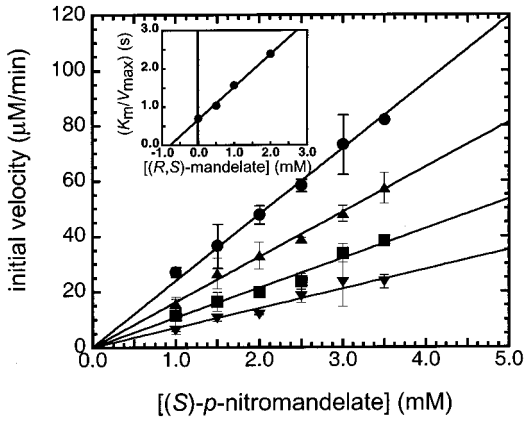

FIGURE 5: Initial velocity curves for the mandelate racemase-catalyzed racemization of (*S*)-*p*-nitromandelate. Assays were conducted at 25 °C in the presence of 0 mM (●), 0.5 mM (▲), 1.0 mM (■), and 2.0 mM (▼) (*R*,*S*)-mandelate. Each point is the average of three determinations. Inset: Replot of the reciprocal slopes obtained from the initial velocity curves (i.e., K_m/V_{max}) as a function of (*R*,*S*)-mandelate concentration. K_i^{app} is equal to 0.78 ± 0.04 mM.

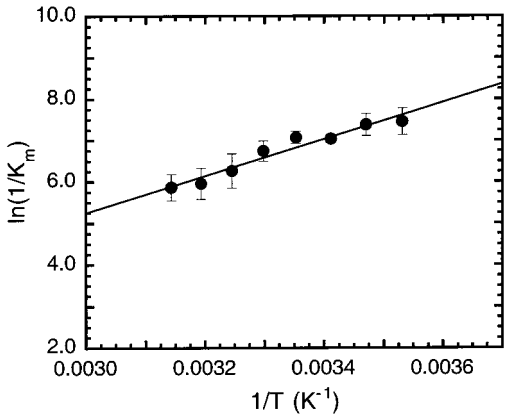

FIGURE 6: Effect of temperature on the reciprocal value of the Michaelis constant ($1/K_m$) for (*R*)-mandelate. Each point represents the average of at least five determinations.

competitive inhibition may be rewritten in terms of the concentrations of (*S*)-mandelate ([(*S*)-man]) and (*R*)-mandelate ([(*R*)-man]) as shown in eq 12.[2] Thus, K_i^{app} is related

$$\frac{v_i}{[E]_t} = \frac{k_{cat}[S]}{[S] + K_m\left[1 + \frac{[(R,S)\text{-man}]}{K_i^{app}}\right]} \quad (11)$$

$$\frac{v_i}{[E]_t} = \frac{k_{cat}[S]}{[S] + K_m\left[1 + \frac{[(S)\text{-man}]}{K_S^{(S)-man}} + \frac{[(R)\text{-man}]}{K_S^{(R)-man}}\right]} \quad (12)$$

to the individual dissociation constants for (*R*)- and (*S*)-mandelate as shown in eq 13. Since the overall equilibrium

$$\frac{[(R,S)\text{-man}]}{K_i^{app}} = \frac{[(S)\text{-man}]}{K_S^{(S)-man}} + \frac{[(R)\text{-man}]}{K_S^{(R)-man}} \quad (13)$$

constant for the interconversion of the enantiomers of mandelate is unity [i.e., $(k_1k_2k_3)/(k_{-1}k_{-2}k_{-3}) = K_{eq} = 1$], the ratio of the dissociation constants may be expressed as a function of individual rate constants as shown in eq 14. Using

$$\frac{k_{-2}}{k_2} = \frac{k_1k_3}{k_{-1}k_{-3}} = \frac{K_S^{(S)-man}}{K_S^{(R)-man}} \quad (14)$$

equilibrium concentrations of (*R*)- and (*S*)-mandelate [i.e., [(*R*)-man] = [(*S*)-man] = [(*R*,*S*)-man]/2], substitution of eq 14 into eq 13 yields eq 15 which relates the apparent inhibition constant for the racemic mixture to the true dissociation constants for (*R*)-mandelate and (*S*)-mandelate.

$$K_i^{app} = \frac{2k_{-2}K_S^{(R)-man}}{k_{-2} + k_2} = \frac{2k_2K_S^{(S)-man}}{k_{-2} + k_2} \quad (15)$$

The rate constants k_2 and k_{-2} are known from the viscosity experiments, and therefore, $K_S^{(R)-man}$ and $K_S^{(S)-man}$ can be calculated.

The value of K_i^{app} is 0.78 ± 0.04 mM (Figure 5). Substitution of this value into eq 15 gives dissociation constants of $K_S^{(R)-man} = 0.89 \pm 0.07$ mM and $K_S^{(S)-man} = 0.69 \pm 0.06$ mM. These values are very similar to the corresponding K_m values reported for (*R*)-mandelate (0.81 ± 0.12 mM) and (*S*)-mandelate (0.62 ± 0.04 mM) (*8*) indicating that, for mandelate racemase, $K_m \approx K_S$. This conclusion is further supported by calculation of the dissociation constants using the rate constants obtained from the viscosity studies ($K_S^{(R)-man} = k_{-1}/k_1 = 0.59 \pm 0.08$ mM and $K_S^{(S)-man} = k_3/k_{-3} = 0.57 \pm 0.07$ mM using k_{-1} and k_3 determined from the slope data in Table 3).

Temperature Effects. Mandelate racemase-catalyzed racemization of (*R*)-mandelate was investigated at temperatures ranging from 10 to 45 °C. The variation of $K_m^{(R)-man}$ with temperature is shown in Figure 6. The enthalpy ($\Delta H_{E\cdot(R)}$) and entropy ($T\Delta S_{E\cdot(R)}$) changes accompanying formation of the enzyme−(*R*)-mandelate complex are −8.9 ± 0.8 kcal/mol and −4.8 ± 0.8 kcal/mol at 25 °C, respectively, corresponding to a free energy ($\Delta G_{E\cdot(R)}$) of −4.1 ± 1.1 kcal/mol at 25 °C.

To determine the activation parameters for conversion of enzyme-bound (*R*)-mandelate to enzyme-bound (*S*)-mandelate, k_2 was determined from viscosity experiments conducted at temperatures ranging from 10 to 45 °C. Values of k_2 were obtained from the reciprocals of the *y*-intercepts on plots of $1/k_{cat}$ versus η_{rel}, and an Eyring plot was used to obtain the corresponding activation parameters (Figure 7). The enthalpy ($\Delta H^{\ddagger}_{E\cdot(R)}$) and entropy ($T\Delta S^{\ddagger}_{E\cdot(R)}$) of activation are 15.4 ± 0.4 kcal/mol and +2.0 ± 0.1 kcal/mol at 25 °C, respectively, corresponding to a free energy of activation ($\Delta G^{\ddagger}_{E\cdot(R)}$) equal to +13.4 ± 0.4 kcal/mol at 25 °C.

The thermodynamic parameters describing the formation of the enzyme−substrate complex in the transition state were

[2] For the determination of K_i^{app}, both (*R*)- and (*S*)-mandelate are present at equilibrium concentrations. It is possible that mandelate racemase behaves like proline racemase (also a two-base racemase) for which the interconversion of two free forms of the enzyme[3] becomes rate-determining as concentrations of substrate and product approach "oversaturation" (i.e., [(*R*)-proline] and [(*S*)-proline] = ~34K_m) (*68*). Scheme 2 would not be valid under such conditions. However, our assay conditions are such that the concentration of (*R*,*S*)-mandelate does not exceed 2 mM (i.e., ~2.5K_m). This is well below the concentrations of substrate and product required to yield the oversaturation kinetics observed for proline racemase.

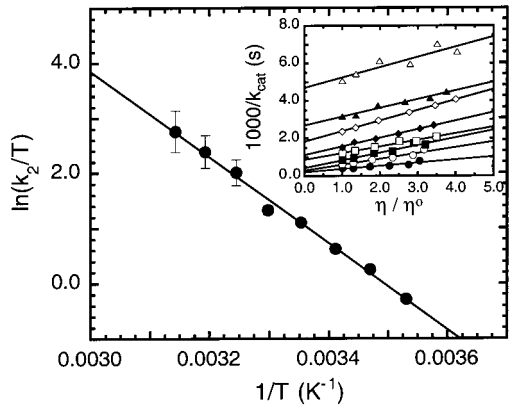

FIGURE 7: Effect of temperature on k_2/T for mandelate racemase acting on (*R*)-mandelate. Error bars represent the error in determining the value of the *y*-intercept from plots of $1/k_{cat}$ as a function of relative solvent viscosity. Inset: Dependence of $1/k_{cat}$ (average of two determinations) on relative solvent viscosity at 10 °C (△), 15 °C (▲), 20 °C (◇), 25 °C (◆), 30 °C (□), 35 °C (■), 40 °C (○), and 45 °C (●) using sucrose as the viscosogen.

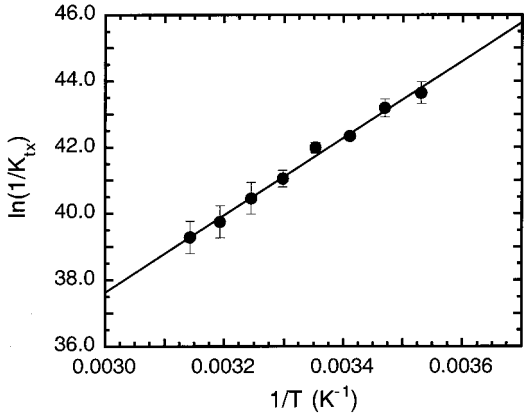

FIGURE 8: Effect of temperature on $1/K_{tx}$ for mandelate racemase acting on (*R*)-mandelate. For each point, K_{tx} was determined from the relationship $K_{tx} = k_{non}/(k_2/K_m)$. Each point represents the average of two determinations.

obtained from a van't Hoff plot (Figure 8) of K_{tx}, where $K_{tx} = k_{non}/(k_2/K_m)$. The nonenzymatic rate constants (k_{non}) were obtained by extrapolation of values determined by Bearne and Wolfenden (*13*) to temperatures between 10 and 45 °C. The enthalpy (ΔH_{tx}) and entropy ($T\Delta S_{tx}$) changes accompanying formation of the enzyme−substrate complex in the transition state are -22.9 ± 0.8 kcal/mol and $+1.8 \pm 0.8$ kcal/mol at 25 °C, corresponding to a free energy of formation for the enzyme−substrate complex in the transition state (ΔG_{tx}) equal to -24.7 ± 1.0 kcal/mol at 25 °C. The thermodynamic parameters describing mandelate racemase catalysis are summarized in Figure 9.

DISCUSSION

The enthalpy and entropy changes that accompany progress along the reaction coordinate of both an enzyme-catalyzed reaction (not involving a covalent enzyme−substrate adduct) and the corresponding nonenzymatic reaction have been described for only a few enzymes including fumarase, ribonuclease A, and carbonic anhydrase (*15*) and more recently cytidine deaminase (*16*). For each of these enzymes, enthalpy is the major contributor to the transition state stabilization free energy, providing additional evidence that

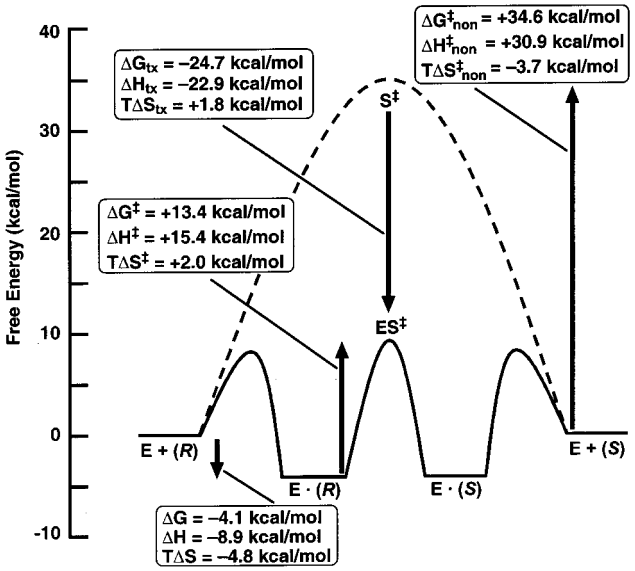

FIGURE 9: Free energy profiles (pH 7.5, 25 °C) for the uncatalyzed (dashed line) and mandelate racemase-catalyzed (solid line) racemization of (*R*)-mandelate [(*R*)] and (*S*)-mandelate [(*S*)]. Energy barriers are drawn to scale using free energies calculated from the rate constants for both the enzymatic reaction (Table 2) and the nonenzymatic reaction (*13*) using the Eyring equation [$k_i = (k_B T/h) \exp(-\Delta G_i^{\ddagger}/RT)$]. ES‡ is the enzyme−substrate complex in the transition state and S‡ is the altered substrate in the transition state for the corresponding nonenzymatic reaction. For simplicity, the "enolic intermediate" (*58*) is not shown on the profile. (Values are calculated for a standard state of 1 M.)

enzymes stabilize reactive intermediates and transition states through numerous synergistic protein−ligand interactions (*17*). It is these interactions that permit proficient enzymes to discriminate between the substrate in the ground state and the altered substrate in the transition state, binding the latter with much greater affinity (*14*, *18*, *19*, *47*−*49*). To extend our knowledge of the thermodynamic changes that contribute to enzyme proficiency, we sought to characterize the changes in enthalpy and entropy occurring during the racemization reaction catalyzed by mandelate racemase. To assess the enthalpy and entropy changes associated with formation of the enzyme−transition state complex, as defined by the virtual dissociation constant K_{tx} (eq 1), it was necessary to confirm that, for mandelate racemase, $K_m = K_S$ and that k_{cat}/K_m and k_{cat} were not limited by substrate binding or product release, respectively.

Viscosity Effects. To accurately estimate the affinity of the enzyme for the altered substrate in the transition state (K_{tx}) using eq 1, either the rate constant describing the chemical step must be determined directly or it must be shown that neither substrate encounter nor product dissociation is rate-determining. The viscosity dependence of k_{cat}/K_m and k_{cat} were used to assess the degree to which substrate association and/or product dissociation were rate-determining for the reaction catalyzed by mandelate racemase. Our observation that the value of k_{cat} in both the $R \rightarrow S$ and $S \rightarrow R$ directions depends on the solvent viscosity is qualitative evidence that the rate of product release (k_3 or k_{-1} in Scheme 1) is not significantly faster than the rate of chemical interconversion of bound enantiomers (k_2, k_{-2}). In addition, a viscosity dependence for k_{cat}/K_m was observed in both the $R \rightarrow S$ and $S \rightarrow R$ directions, suggesting that substrate binding is also partially rate-determining for mandelate racemase catalysis.

Interestingly, the values of k_1 and k_{-3} are about 1−2 orders of magnitude lower than typical values of diffusive association rate constants for enzymatic reactions (*27*). Such low values for association rate constants may arise because the conformation of the unliganded enzyme required for substrate binding exists as a rare form (*35*),[3] extensive desolvation of both the substrate and the active site is required (*35*, *50*), nonproductive substrate binding occurs (*22*), or a rate-determining conformational change occurs after substrate binding but prior to the chemical step (*40*, *51*, *52*). For example, substrate binding and concomitant chelation of the active site Mg^{2+} may be accompanied by slow displacement of the water molecules coordinated to the metal ion (and possibly a concomitant conformational change) which may limit the apparent rate of association. X-ray crystal structures of mandelate racemase have revealed the presence of a flexible loop (residues 19−30) which is closed over the active site when substrate is bound (*5*). Viscosity effects may arise because the opening and closing motions of this flexible loop contribute to the physical barrier which limits external steps. Rapid opening and closing motions have been reported for the catalytically essential mobile loops found in triosephosphate isomerase (*53*, *54*) and *Yersinia* protein tyrosine phosphatase (*55*), and the rates of these motions are compatible with on rates approaching the diffusion limit. For triosephosphate isomerase, the loop-open form of the unliganded enzyme is favored over the loop-closed form by 1.8 kcal/mol (*53*). If mandelate racemase behaves like these enzymes, then the loop-open form would not constitute a rare form of the enzyme and it is unlikely that loop motions would limit the apparent rate of substrate association. However, release of product from mandelate racemase may well be limited by the rate of loop opening. The loop-closed form of triosephosphate isomerase is favored by 1.5−2.8 kcal/mol when ligand is bound (*53*), and loop opening has been suggested to be responsible for the external kinetic step that limits k_{cat} for other enzymes including staphylococcal nuclease (*38*), dihydrofolate reductase (*56*), and orotate phosphoribosyltransferase (*52*, *57*).

The partial viscosity dependence of mandelate racemase catalysis at 25 °C was used to directly estimate the rate constants (Table 3) for the kinetic mechanism shown in Scheme 1. The free energy barrier for racemization of bound substrate, in both reaction directions, is approximately 1 kcal/mol greater than the free energy barriers for dissociation of bound ligands, indicating that, for mandelate racemase, enzyme−substrate or enzyme−product dissociation is not significantly favored over proton abstraction. For example, under initial velocity conditions in the $R \rightarrow S$ direction, approximately 85% of the enzyme−product complex goes on to form free product. This observation is in agreement with the prediction of Gerlt and Gassman (*58*) that, for enzyme-catalyzed concerted general acid−general base reactions, the rate of enolization of the substrate carbon acid is expected to be similar to the rates of substrate binding and/or product release. Because the sum of the rate constants for the chemical steps (i.e., $k_{-2} + k_2$) is similar in magnitude to the rate constants for product dissociation (k_3 or k_{-1}), the observed value of k_{cat} underestimates k_2 by approximately 30% in either direction.[4] The efficiency of mandelate racemase catalysis, therefore, is limited in both directions as much by the diffusion-controlled external steps as it is by the rate of chemical conversion of the bound substrate to bound product. Given these physical constraints, mandelate racemase may be regarded as a *nearly* perfect enzyme. Indeed, there is little evolutionary pressure for an enzyme to evolve such that it can catalyze a chemical step faster than the rates for the physical exchange of substrate or product with solvent (*59*, *60*). Other enzymes such as carbonic anhydrase (*61*) and β-lactamase (*42*), which are also only *partially* limited by the rates of diffusion, are considered to have reached the limit of their evolution, such that no further improvements in the rate of their chemical steps can increase their overall enzyme efficiency.

Substrate Binding. The dissociation constants for (*R*)- and (*S*)-mandelate were determined using a kinetic approach in which (*R*,*S*)-mandelate was used to competitively inhibit the racemization of the alternative substrate, (*S*)-*p*-nitromandelate. The inhibition constant for (*R*,*S*)-mandelate was subsequently used to calculate the true substrate dissociation constants. The 10-fold reduction in k_{cat}/K_m for (*S*)-*p*-nitromandelate, relative to that for (*S*)-mandelate, was not initially expected since the electron-withdrawing bromo and chloro para-substituted mandelic acids have values of k_{cat}/K_m that are greater than that observed for mandelate (*1*). However, the absence of saturation kinetics at concentrations of (*S*)-

[3] Proline racemase[2] has been reported to exist in two forms, each binding only one of the enantiomeric substrates (*68*). These two enzyme forms are presumed to differ in the protonation states of their active site bases which catalyze proton abstraction. If a similar scenario held for mandelate racemase, then at low substrate concentrations, approximately 50% of the enzyme would be available for reaction with a single enantiomer. This hardly constitutes a rare form of the enzyme, and at low substrate concentrations, proline racemase is not limited by interconversion of the two enzyme forms (*68*). An alternative hypothesis is that the free enzyme exists in an equilibrium between a loop-open and a loop-closed form, with the former species being the rare form. However, this possibility also seems unlikely for reasons discussed in the text.

[4] Because proton abstraction is not solely rate-determining, the observed deuterium kinetic isotope effects, reported previously (*7*, *20*), likely underestimate the intrinsic deuterium isotope effect (*69*). The values of the rate constants determined in the present study can be used to estimate the intrinsic deuterium isotope effect for the forward and reverse enzyme-catalyzed reactions using eqs 17 and 18, derived following the method described by Northrop (*70*) and assuming that the forward and reverse intrinsic kinetic isotope effects are equal (i.e., $k_{2H}/k_{2D} = k_{-2H}/k_{-2D}$).

$$\frac{V_H^{R\rightarrow S}}{V_D^{R\rightarrow S}} = \frac{\frac{k_{2H}}{k_{2D}} + \left(\frac{k_{-2}+k_2}{k_3}\right)^H}{\left(\frac{k_{-2}+k_2}{k_3}\right)^H + 1} \quad (17)$$

$$\frac{V_H^{S\rightarrow R}}{V_D^{S\rightarrow R}} = \frac{\frac{k_{-2H}}{k_{-2D}} + \left(\frac{k_{-2}+k_2}{k_{-1}}\right)^H}{\left(\frac{k_{-2}+k_2}{k_{-1}}\right)^H + 1} \quad (18)$$

The values of V_H/V_D are equal to 3.20 ± 0.11 and 3.56 ± 0.12 for catalysis in the $R \rightarrow S$ and $S \rightarrow R$ directions, respectively (*20*). Substitution of these values and the values for the rate constants from Table 3 into eqs 17 and 18 gives $k_{2H}/k_{2D} = 4.1 \pm 0.5$ and $k_{-2H}/k_{-2D} = 4.6 \pm 0.5$ for catalysis in the $R \rightarrow S$ and $S \rightarrow R$ directions. Interestingly, these values are less than those expected for "normal" deuterium isotope effects [$k_H/k_D = 6-10$ (*69*)] but are consistent with the occurrence of late transition states for enzyme-catalyzed proton abstraction in both the forward and reverse reactions (*58*, *69*).

p-nitromandelate up to 15 mM indicates that binding of (*S*)-*p*-nitromandelate is unfavorable, accounting for the decreased k_{cat}/K_m value.

We have shown that, for mandelate racemase, the Michaelis constant (K_m) is equal to the dissociation constant (K_S). This result agrees with previous experiments in which K_S was calculated from protection experiments using the irreversible inactivator (*R*,*S*)-phenylglycidate (*62*) and magnetic resonance titrations (*63*). In addition, our values for the rate constants obtained using the viscosity variation method also support this conclusion. Two sets of conditions will satisfy eq 16 such that $K_m^{(R)-man} \approx k_{-1}/k_1 = K_S^{(R)-man}$. First, the chemical step may be completely rate-determining in the forward and reverse directions (i.e., $k_{-1} \gg k_2$, k_{-2} and $k_3 \gg k_2$, k_{-2}). However, this scenario is not compatible with the partial viscosity dependence exhibited by mandelate racemase, which indicates that the rates of substrate and product dissociation are similar to the rate of chemical interconversion of bound substrate and product. Second, if the off rates are equal for both substrates (i.e., $k_{-1} \approx k_3$) and the internal equilibrium constant (k_2/k_{-2}) is approximately unity, then $K_m \approx K_S$. The rate constants shown in Table 1 confirm that this is the case for mandelate racemase.

$$K_m^{(R)-man} = \frac{k_{-1}k_{-2} + k_{-1}k_3 + k_2k_3}{k_1(k_{-2} + k_2 + k_3)} \qquad (16)$$

Changes in Enthalpy and Entropy during Catalysis. We have investigated the temperature dependence of K_m and k_2 to obtain an estimate of the enthalpic and entropic contributions to the free energy of substrate binding in the ground state and to the activation free energy for the chemical step [conversion of E·(*R*)-man to E·(*S*)-man] in the $R \rightarrow S$ direction (data are summarized in Table 3 and Figure 9). Substrate binding ($1/K_m$) is accompanied by an enthalpy release (−8.9 kcal/mol), consistent with the formation of noncovalent interactions between the enzyme and the substrate in the enzyme−substrate complex. In addition, substrate binding is accompanied by a loss of entropy (−4.8 kcal/mol at 25 °C). For the chemical step, a substantial enthalpy of activation is associated with catalysis (+15.4 kcal/mol) which is similar to the enthalpy of activation recently reported for cytidine deaminase (*16*). Although this enthalpy change is large relative to values of 9−13 kcal/mol reported for other enzymes (*17*), it does, nevertheless, represent an impressive 15 kcal/mol decrease in activation enthalpy relative to the nonenzymatic reaction [$\Delta H^{\ddagger} = +30.9$ kcal/mol (*13*)]. This $\Delta\Delta H^{\ddagger}$ is well within the range exhibited by other enzymes ($\Delta\Delta H^{\ddagger} = 7-33$ kcal/mol) (*16*, *17*). Interestingly, unlike cytidine deaminase (*16*), the release of enthalpy accompanying substrate binding does not match the enthalpy of activation associated with the subsequent chemical step. The free energy of activation for the enzymatic reaction is accompanied by a favorable gain in entropy (+2.0 kcal/mol) while a loss of entropy is associated with the nonenzymatic reaction ($T\Delta S^{\ddagger} = -3.7$ at 25 °C). The positive difference in activation entropies (i.e., $T\Delta\Delta S^{\ddagger} = +5.7$ kcal/mol) between the enzymatic and nonenzymatic reactions is in qualitative agreement with the prediction of Gerlt and Gassman (*58*) that the intrinsic entropy of activation for a concerted enzymatic reaction is expected to be less negative than the corresponding base-catalyzed nonenzymatic reaction, thereby providing a mechanism for lowering the free energy of activation on the enzyme. Such a positive $\Delta S^{\ddagger}$ for the enzyme-catalyzed reaction could arise from either an enzyme conformational change, as implicated by the viscosity variation results, and/or changes in solvation during the reaction (*64*).

Thermodynamics of Transition State Affinity. After a substrate is bound by an enzyme, the affinity of the enzyme for the substrate increases by a factor proportional to the rate enhancement produced by that enzyme (*14*, *18*, *19*). We have used the method of viscosity variation to determine the rate constant (k_2) corresponding to the chemical conversion of bound (*R*)-mandelate into (*S*)-mandelate, thereby permitting us to accurately estimate the value of the true rate enhancement (k_2/k_{non}) and calculate the virtual dissociation constant for the enzyme−substrate complex in the transition state (K_{tx}). Values of K_{tx} were estimated over a range of temperatures by dividing the rate constant for the reaction in the absence of enzyme [k_{non}, obtained by extrapolation of the data of Bearne and Wolfenden (*13*)] by the apparent second-order rate constant k_2/K_m for the enzyme-catalyzed reaction at the same temperature. It is important to note that calculation of K_{tx} using k_{cat}/K_m rather than k_2/K_m would result in an underestimation of the affinity of the enzyme for the altered substrate in the transition state. The variation of $1/K_{tx}$ with temperature (Figure 8) indicates that enthalpy is the major contributor to transition state stabilization, providing −22.9 kcal/mol of energy to the apparent binding free energy of the altered substrate in the transition state. This substantial release of energy is compatible with the development of enhanced hydrogen bonding, electrostatic interactions, and nonpolar interactions in the enzyme−transition state complex (*17*). The importance of such interactions in mandelate racemase catalysis has been suggested by X-ray crystal structures of bound ground-state ligands (*5*) and site-directed mutagenesis experiments (*6*−*8*, *13*, *65*, *66*).

The entropy change associated with *binding* of the altered substrate in the transition state is estimated to be $T\Delta S_{tx} = +1.8$ kcal/mol at 25 °C. Positive entropies for transition state binding have been reported for fumarase (*15*) and cytidine deaminase (*16*). Whether the positive entropic component of transition state stabilization by mandelate racemase arises from the release of an ordered water molecule from the active site as is believed to be the case for cytidine deaminase (*16*, *67*) or from more general changes in solvation and enzyme conformation is not presently clear.

Thus, mandelate racemase stabilizes the transition state for proton abstraction (ΔG_{tx}) by reducing the enthalpy of activation (by ΔH_{tx}) and increasing the entropy of activation (by ΔS_{tx}) relative to the nonenzymatic reaction. Molecular interactions between mandelate racemase and its altered substrate in the transition state appear to be maximized to the extent that diffusion-dependent processes are partially rate-determining, suggesting that mandelate racemase has evolved close to the limit of its catalytic proficiency.

ACKNOWLEDGMENT

We express our thanks to Shauna Drover for conducting the resolution of *p*-nitromandelate. (S.D. was supported by an NSERC summer undergraduate research award.)

REFERENCES

1. Hegeman, G. D., Rosenberg, E. Y., and Kenyon, G. L. (1970) *Biochemistry 9*, 4029−4036.
2. Kenyon, G. L., and Hegeman, G. D. (1979) *Adv. Enzymol. Relat. Areas Mol. Biol. 50*, 325−360.
3. Kenyon, G. L., Gerlt, J. A., Petsko, G. A., and Kozarich, J. W. (1995) *Acc. Chem. Res. 28*, 178−186.
4. Powers, V. M., Koo, C. W., Kenyon, G. L., Gerlt, J. A., and Kozarich, J. W. (1991) *Biochemistry 30*, 9255−9263.
5. Neidhart, D. J., Howell, P. L., Petsko, G. A., Powers, V. M., Li, R. S., Kenyon, G. L., and Gerlt, J. A. (1991) *Biochemistry 30*, 9264−9273.
6. Landro, J. A., Kallarakal, A. T., Ransom, S. C., Gerlt, J. A., Kozarich, J. W., Neidhart, D. J., and Kenyon, G. L. (1991) *Biochemistry 30*, 9274−9281.
7. Mitra, B., Kallarakal, A. T., Kozarich, J. W., Gerlt, J. A., Clifton, J. G., Petsko, G. A., and Kenyon, G. L. (1995) *Biochemistry 34*, 2777−2787.
8. St. Maurice, M., and Bearne, S. L. (2000) *Biochemistry 39*, 13324−13335.
9. Gerlt, J. A., Kenyon, G. L., Kozarich, J. W., Neidhart, D. C., and Petsko, G. A. (1992) *Curr. Opin. Struct. Biol. 2*, 736−742.
10. Babbitt, P. C., Hasson, M. S., Wedekind, J. E., Palmer, D. R., Barrett, W. C., Reed, G. H., Rayment, I., Ringe, D., Kenyon, G. L., and Gerlt, J. A. (1996) *Biochemistry 35*, 16489−16501.
11. Babbitt, P. C., and Gerlt, J. A. (1997) *J. Biol. Chem. 272*, 30591−30594.
12. Gerlt, J. A. (1998) in *Bioorganic Chemistry: Peptides and Proteins* (Hecht, S. M., Ed.) pp 279−311, Oxford University Press, New York.
13. Bearne, S. L., and Wolfenden, R. (1997) *Biochemistry 36*, 1646−1656.
14. Radzicka, A., and Wolfenden, R. (1995) *Science 267*, 90−93.
15. Bearne, S. L., and Wolfenden, R. (1995) *J. Am. Chem. Soc. 117*, 9588−9589.
16. Snider, M. J., Gaunitz, S., Ridgway, C., Short, S. A., and Wolfenden, R. (2000) *Biochemistry 39*, 9746−9753.
17. Wolfenden, R., Snider, M. J., Ridgway, C., and Miller, B. (1999) *J. Am. Chem. Soc. 121*, 7419−7420.
18. Wolfenden, R. (1972) *Acc. Chem. Res. 5*, 10−18.
19. Wolfenden, R. (1974) *Mol. Cell. Biochem. 3*, 207−211.
20. Whitman, C. P., Hegeman, G. D., Cleland, W. W., and Kenyon, G. L. (1985) *Biochemistry 24*, 3936−3942.
21. Dale, M. P., Kopfler, W. P., Chait, I., and Byers, L. D. (1986) *Biochemistry 25*, 2522−2529.
22. Simopoulos, T. T., and Jencks, W. P. (1994) *Biochemistry 33*, 10375−10380.
23. Li, Y., Feng, L., and Kirsch, J. F. (1997) *Biochemistry 36*, 15477−15488.
24. Steyaert, J., Wyns, L., and Stanssens, P. (1991) *Biochemistry 30*, 8661−8665.
25. Stratton, J. R., Pelton, J. G., and Kirsch, J. F. (2001) *Biochemistry 40*, 10411−10416.
26. Mattei, P., Kast, P., and Hilvert, D. (1999) *Eur. J. Biochem. 261*, 25−32.
27. Alberty, R. A., and Hammes, G. G. (1958) *J. Am. Chem. Soc. 62*, 154−159.
28. Bearne, S. L., St. Maurice, M., and Vaughan, M. D. (1999) *Anal. Biochem. 269*, 332−336.
29. Westkaemper, R. B., and Hanzlik, R. P. (1981) *Arch. Biochem. Biophys. 208*, 195−204.
30. Newman, P. (1981) *Optical resolution procedures for chemical compounds*, Vol. 2, Optical Resolution Information Center, Riverdale, NY.
31. Sharp, T. R., Hegeman, G. D., and Kenyon, G. L. (1979) *Anal. Biochem. 94*, 329−334.
32. Jencks, W. P., and Regenstein, J. (1968) in *Handbook of Biochemistry* (Sober, H. A., Ed.) pp J150−J189, The Chemical Rubber Co., Cleveland, OH.
33. Bubnik, Z., Kadlec, P., Urban, D., and Bruhns, M. (1995) in *Sugar Technologists Manual: Chemical and Physical Data for Sugar Manufacturers and Users*, p 164, Bartens, Berlin.
34. Bazelyansky, M., Robey, E., and Kirsch, J. F. (1986) *Biochemistry 25*, 125−130.
35. Blacklow, S. C., Raines, R. T., Lim, W. A., Zamore, P. D., and Knowles, J. R. (1988) *Biochemistry 27*, 1158−1167.
36. Brouwer, A. C., and Kirsch, J. F. (1982) *Biochemistry 21*, 1302−1307.
37. Caldwell, S. R., Newcomb, J. R., Schlecht, K. A., and Raushel, F. M. (1991) *Biochemistry 30*, 7438−7444.
38. Hale, S. P., Poole, L. B., and Gerlt, J. A. (1993) *Biochemistry 32*, 7479−7487.
39. Hardy, L. W., and Kirsch, J. F. (1984) *Biochemistry 23*, 1275−1282.
40. Kurz, L. C., Weitkamp, E., and Frieden, C. (1987) *Biochemistry 26*, 3027−3032.
41. Pocker, Y., and Janjic, N. (1987) *Biochemistry 26*, 2597−2606.
42. Christensen, H., Martin, M. T., and Waley, S. G. (1990) *Biochem. J. 266*, 853−861.
43. Goldberg, J. M., and Kirsch, J. F. (1996) *Biochemistry 35*, 5280−5291.
44. Adams, J. A., and Taylor, S. S. (1992) *Biochemistry 31*, 8516−8522.
45. Stone, S. R., and Morrison, J. F. (1988) *Biochemistry 27*, 5493−5499.
46. Sampson, N. S., and Knowles, J. R. (1992) *Biochemistry 31*, 8488−8494.
47. Lienhard, G. E. (1973) *Science 180*, 149−154.
48. Polanyi, M. (1921) *Z. Elektrochem. 27*, 143−150.
49. Wolfenden, R. (1976) *Annu. Rev. Biophys. Bioeng. 5*, 271−306.
50. Bartlett, P. A., and Marlowe, C. K. (1987) *Biochemistry 26*, 8553−8561.
51. Hoggett, J. G., and Kellett, G. L. (1976) *Eur. J. Biochem. 68*, 347−353.
52. Wang, G. P., Cahill, S. M., Liu, X., Girvin, M. E., and Grubmeyer, C. (1999) *Biochemistry 38*, 284−295.
53. Williams, J. C., and McDermott, A. E. (1995) *Biochemistry 34*, 8309−8319.
54. Derreumaux, P., and Schlick, T. (1998) *Biophys. J. 74*, 72−81.
55. Juszczak, L. J., Zhang, Z. Y., Wu, L., Gottfried, D. S., and Eads, D. D. (1997) *Biochemistry 36*, 2227−2236.
56. Falzone, C. J., Wright, P. E., and Benkovic, S. J. (1994) *Biochemistry 33*, 439−442.
57. Wang, G. P., Lundegaard, C., Jensen, K. F., and Grubmeyer, C. (1999) *Biochemistry 38*, 275−283.
58. Gerlt, J. A., and Gassman, P. G. (1993) *J. Am. Chem. Soc. 115*, 11552−11568.
59. Albery, W. J., and Knowles, J. R. (1977) *Angew. Chem., Int. Ed. Engl. 16*, 285−293.
60. Burbaum, J. J., Raines, R. T., Albery, W. J., and Knowles, J. R. (1989) *Biochemistry 28*, 9293−9305.
61. Hasinoff, B. B. (1984) *Arch. Biochem. Biophys. 233*, 676−681.
62. Fee, J. A., Hegeman, G. D., and Kenyon, G. L. (1974) *Biochemistry 13*, 2533−2538.
63. Maggio, E. T., Kenyon, G. L., Mildvan, A. S., and Hegeman, G. D. (1975) *Biochemistry 14*, 1131−1139.
64. Laidler, K. J., and Peterman, B. F. (1979) *Methods Enzymol. 63*, 234−257.
65. Kallarakal, A. T., Mitra, B., Kozarich, J. W., Gerlt, J. A., Clifton, J. G., Petsko, G. A., and Kenyon, G. L. (1995) *Biochemistry 34*, 2788−2797.
66. Landro, J. A., Gerlt, J. A., Kozarich, J. W., Koo, C. W., Shah, V. J., Kenyon, G. L., Neidhart, D. J., Fujita, S., and Petsko, G. A. (1994) *Biochemistry 33*, 635−643.
67. Snider, M. J., and Wolfenden, R. (2001) *Biochemistry 40*, 11364−11371.
68. Fisher, L. M., Albery, W. J., and Knowles, J. R. (1986) *Biochemistry 25*, 2529−2537.
69. Jencks, W. P. (1987) *Catalysis in Chemistry and Enzymology*, pp 243−281, Dover Publications, New York.
70. Northrop, D. B. (1975) *Biochemistry 14*, 2644−2651.

BI016044H